ELSEVIER

Journal of Organometallic Chemistry 554 (1998) 87–103

Journal of Organometallic Chemistry

Excited states and emission spectroscopy of organometallic compounds interpreted by time-dependent theory

Ana Acosta, Jeffrey I. Zink *

Department of Chemistry and Biochemistry, University of California, Los Angeles, CA 90095, USA

Received 21 January 1997; received in revised form 14 April 1997

Abstract

Luminescence spectra of organometallic molecules in crystals or glasses are discussed and interpreted by using the time-dependent theory of electronic spectroscopy. Emphasis is placed on determining bond length and bond angle changes (excited-state distortions) between the ground and excited electronic states. The physical meaning of the dynamic processes and the molecular properties are described and illustrated with both theoretical calculations and experimental spectra. The discussion begins with spectra involving only one displaced normal mode, and continues with the effects of multiple normal modes. Both common features and unusual effects (the 'Beat' and the 'MIME') are described and interpreted. Finally, the effects of normal mode coupling and of electronic state coupling are briefly described. © 1998 Elsevier Science S.A.

Keywords: Excited states; Emission spectroscopy; Time-dependent theory; Organometallic compounds

1. Introduction

Luminescence spectroscopy (fluorescence if the transition is spin-allowed, phosphorescence if it is spin-forbidden) has long been recognized as an important method for determining excited-state energies [1–6]. Because luminescent molecules in condensed media usually emit from the lowest excited state of a given spin multiplicity (Kasha's rule [7]), and because this state is also usually responsible for photochemical activity, luminescence spectra (together with lifetime data) can yield fundamental understanding about both photochemical and photophysical processes. Luminescence spectra can provide much more information than just an excited-state energy. For example, the width of the spectrum directly provides information about the steepest slope of the potential surface and thus about the femtosecond dynamics. Vibronic structure in the spectrum provides information about the bond length and angle changes between the ground and excited states. Intensities provide information about vibrational coupling and electronic state coupling. These aspects of excited states form the subject of this paper. Our goal is to present luminescence spectroscopy from a point of view that emphasizes the physical picture of the dynamic process. This point of view is illustrated with both simple models and with experimental examples. Our intent is to 'train the eye' such that the chemist can interpret emission spectra and extract from them the structural and photophysical details that they reveal about the molecule.

The recent development that makes possible a simple interpretation of electronic spectroscopy is the time-dependent theory [8–10]. The time-dependent theory provides a powerful quantitative calculational method and an intuitive physical picture for interpreting how a molecule reacts upon the absorption or emission of light. The key aspect of the physical picture is the motion of a wave packet on a potential surface. Before we discuss electronic transitions, we will briefly review the physical picture of molecular motions. Potential energy surfaces such as those shown in Fig. 1 form the bases of this description. The surface is a plot of the energy of the molecule versus a normal coordinate of vibration. A nonlinear molecule containing N atoms has $3N$-6 vibrational normal coordinates; we will assume that they are separable and nondegenerate, and that a cross-section of the multidimensional surface can be

* Corresponding author.

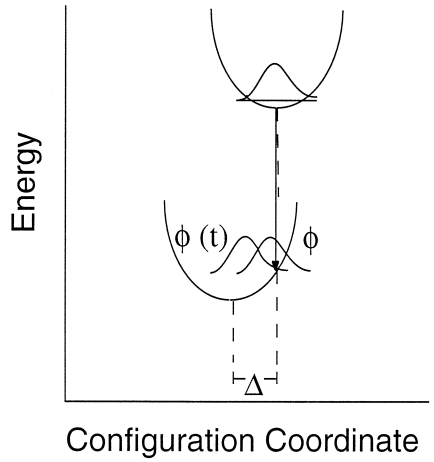

Fig. 1. Cross-section of ground- and excited-state potential surfaces along a specific normal coordinate. The figure illustrates the emission experiment where the vertical transition places the wave packet on the ground-state potential surface. This wave packet then propagates. The ground- and excited-state potential surfaces are displaced by a distortion Δ.

used to represent one specific vibrational mode. The molecular motions can be represented by the motions of a ball on the potential surface. If the ball is placed on the surface at a point away from the minimum (for example, where the arrow points in Fig. 1), it will have nonzero potential energy and will begin to roll down the slope, lose potential energy and gain kinetic energy. The motion along the normal coordinate represents a change in the bond distances and angles in the molecule. The ball will roll past the minimum of the surface (which represents the bond lengths and angles of the molecule when it is at equilibrium in the electronic state corresponding to the surface) and then roll up the other side where it momentarily will come to rest. This position represents the opposite extreme of bond length and angles from that of the initial position. Then it will roll back down, retracing its path until it comes to rest at its initial position. The amount of time that it takes to make one round trip corresponds to one vibrational period.

In electronic spectroscopy, the emission (or absorption) of a photon causes a transition from one electronic state (one potential surface) to another. The transition is vertical (it takes place with no change in the bond lengths or angles) and thus occurs from the position of the minimum of the initial surface to the position vertically below (or above) it on the final surface. According to the time-dependent picture of spectroscopy, the photon creates a wave packet (the initial vibrational wavefunction multiplied by the transition dipole moment) that is placed on the final surface. Once there it propagates, or moves according to the time-dependent Schrödinger equation (similar to the motion of the ball in the above example). In the emission experiment, the initial wave packet starts on the upper (excited electronic state) surface and makes a vertical transition to the ground electronic state surface, propagating on the latter one. This propagating wave packet is called the time-dependent wave packet or $\phi(t)$. In electronic emission or absorption spectroscopy, the quantity of interest is the time-dependent overlap of the initial wave packet with the time-dependent wave packet, $\langle \phi | \phi(t) \rangle$. The Fourier transform of this overlap in the time domain gives us the spectrum in the frequency domain. In this paper, we will concentrate on emission spectra because only two potential surfaces, the ground state surface and the surface for the lowest excited state of a given spin multiplicity (Kasha's Rule) are needed. Absorption spectroscopy is treated in a very similar manner, and for uncoupled electronic states, the same two surfaces are used. The major difference is that the initial state is the ground state and the final state (on which the wave packet propagates) is the excited state. However, there are many excited states frequently near each other, and multiple potential surfaces may have to be used.

2. Summary of time-dependent theory

The mathematical details of the theory have been discussed previously [8–12] (for an introductory overview, see Ref. [13]), and only a brief discussion of the general aspects will be given here. The emission spectrum is governed by the motion of the initial wave packet, $\phi = \phi(t = 0)$ on the multidimensional ground electronic state potential surface. This surface is, in general, displaced relative to the excited-state surface along normal vibrational coordinates, and has a different functional form from that of the excited-state surface. The wave packet is, in general, not an eigenfunction of the ground state surface and develops in time according to the time-dependent Schrödinger equation. The emission spectrum is given by [8–10]:

$$I(\omega) = C\omega^3 \int_{-\infty}^{+\infty} \exp(i\omega t) \left\{ \langle \phi | \phi(t) \rangle \times \exp\left(-\Gamma^2 t^2 + \frac{iE_{00}}{\hbar} t \right) \right\} \mathrm{d}t \quad (1)$$

where $I(\omega)$ is the intensity in photons per unit volume per unit time at frequency of emitted radiation ω, C is a constant, and $\langle \phi | \phi(t) \rangle$ is the overlap of the initial wave packet, $\phi = \phi(t = 0)$ with the time-dependent wave packet $\phi(t)$. Γ is a phenomenological damping factor and E_{00} is the energy of the origin of the electronic transition. The physical meaning and spectroscopic consequences of these parameters are discussed in Section 3.

The time dependence of the wave packet evolving on a potential surface can be numerically determined by

using the split operator technique of Feit et al. [11]. The time-dependent Schrödinger equation is

$$i\frac{\partial\phi}{\partial t} = -\frac{1}{2M}\nabla^2\phi + V(Q)\,\phi \qquad (2)$$

where $\nabla^2 = \partial^2/\partial x^2 + \partial^2/\partial y^2$ and $V(Q)$ is the potential energy surface. The wavefunction at a time $t+\Delta t$ is [11]:

$$\phi(t+\Delta t) = \exp\left(\left(\frac{i\Delta t}{4M}\right)\nabla^2\right)\exp(-i\Delta t V) \times \exp\left(\left(\frac{i\Delta t}{4M}\right)\nabla^2\right)\phi(Q,t=0) + O\left[(\Delta t)^3\right] \qquad (3)$$

The dominant error term is third order in Δt. The initial wavefunction $\phi(Q,t)$ at $t=0$ is normally the lowest energy eigenfunction of the initial state of the spectroscopic transition. The value of the wavefunction at incremental time intervals Δt is calculated by using Eq. (3) for each point on the (Q) grid. The autocorrelation function is then calculated at each time interval and the resulting $\langle\phi|\phi(t)\rangle$ is Fourier transformed according to Eq. (1) to give the emission spectrum.

The two most important choices that must be made in the numerical calculations are the size of the time steps and the size of the computational grid. The smaller the increment in the time steps and the smaller the spacing between the grid points, the greater the accuracy in the calculation. General criteria for initial choices have been published [12,13].

For many emission spectra of organometallic molecules, several simplifying approximations can be made without severe loss of accuracy. If it is assumed that (a) the force constants are the same in both ground and excited states, (b) the potential surfaces are harmonic, (c) the transition dipole moment, μ, is constant, and, (d) the normal coordinates are not mixed in the excited state, then the overlap, $\langle\phi|\phi(t)\rangle$ in emission or absorption has a simple form. None of these assumptions are requirements of the time-dependent theory. When the vibrational frequencies in the excited state are not known (as is usually the case), the assumption of no change in force constant between surfaces can be used, but it does not introduce an error exceeding 10% [14]. The harmonic approximation can often be used because the spectroscopic action usually takes place deep in the potential wells where anharmonic effects are small. Under the assumptions described above, the overlap for one specific normal mode (kth) has the simple form

$$\langle\phi_k|\phi_k(t)\rangle = \exp\left\{-\frac{\Delta_k^2}{2}(1-\exp(-i\omega_k t) - \frac{i\omega_k t}{2}\right\} \qquad (4)$$

where ω_k and Δ_k are, respectively, the vibrational frequency in cm^{-1} and the displacement of the kth normal mode. The magnitude of damped overlap, $|\langle\phi|\phi(t)\rangle\exp(-\Gamma^2 t^2)|$ is plotted in all of our figures of $\langle\phi|\phi(t)\rangle$ in the following discussion. The overlap is a maximum at $t=t_0$ and decreases as the wave packet moves away from its initial position. It reaches a minimum when the wave packet is far away from the Franck Condon region. But when it comes back to where it started, the overlap increases once again, giving a recurrence of the overlap, which will not have the same relative intensity as when it started because of the damping factor, Γ. This recurrence in the time domain corresponds to one vibrational period of the mode, and in a structured emission spectrum, the recurrence is related to the separation between the vibronic peaks that form the progression in that vibrational mode. In most transition metal and organometallic compounds, many modes are displaced. In the case of many displaced normal modes, the total overlap is the product of the overlaps of the k individual modes

$$\langle\phi|\phi(t)\rangle = \prod_k \langle\phi_k|\phi_k(t)\rangle \qquad (5)$$

The electronic emission spectrum in the frequency domain is the Fourier transform of the overlap in the time domain (Eq. (1)).

No commercial software to carry out these calculations is available at the time of writing. The simplest way to get started would be to calculate overlap as a function of time following Eq. (4), and then to Fourier transform the autocorrelation function as shown in Fig. 1. Fast Fourier transform algorithms are commonly available. To carry out the more accurate calculations involving propagation of the wave packet, Eq. (3) must be implemented as discussed in Ref. [11]. In both cases, the required inputs are the potential surfaces (that frequently can be approximated as harmonic oscillator surfaces defined by the observed vibrational frequencies from the infrared or Raman spectra), the E_{00} determined from the electronic spectrum and Γ determined by the vibronic band width. The variables to be fit are the Δ's, the displacements of the excited surface relative to the ground state surface along the normal coordinates. For uncoupled vibrations and one electronic excited state, a typical calculation requires tens of seconds on a PC.

3. Interpretation of emission spectra

In this section, we will illustrate how to interpret spectra using the time-dependent theory. Our emphasis will be on the physical meaning and on how the different properties of the potential surfaces are manifested in experimental spectra. To do this, we will use calculated spectra in which only one specific parameter is changed at a time. These spectra will serve as pedagogical examples of what an 'ideal' spectrum would look like.

An understanding of the dynamic processes that take place will result in the 'trained eye' that is necessary to both interpret real spectra and to assign the distortions the molecule undergoes when excited. Relevant experimental examples taken from our own work are referenced, and in some instances discussed in each section.

3.1. Emission spectra with one displaced mode

The main features of any spectrum (in the frequency domain) are determined by features present in the overlap (in the time domain) of the initial wave packet with the propagating one. To see how the dynamics of this overlap of two wave packets shape our spectra, we will start with simple examples.

The shape of the electronic potential surface is frequently parabolic. The first feature that we will examine for spectroscopic consequences is the steepness of its walls. In the specific dimension being examined, the higher the vibrational frequency, the steeper the walls. The steepness becomes greater as we go up its walls, and is less if we move down. The slope of this 'wall of the well' will determine how long the initial wave packet will overlap with the propagating one. If the wave packet is born on a very steep part of the well, it will move away from its initial position faster than it would if it were on a shallow slope, and the result is a sharp drop of the overlap in the plot of $\langle \phi | \phi(t) \rangle$ (Fig. 2). The closer the wave packet is to the bottom of the surface, the less steep the slope and the longer the time

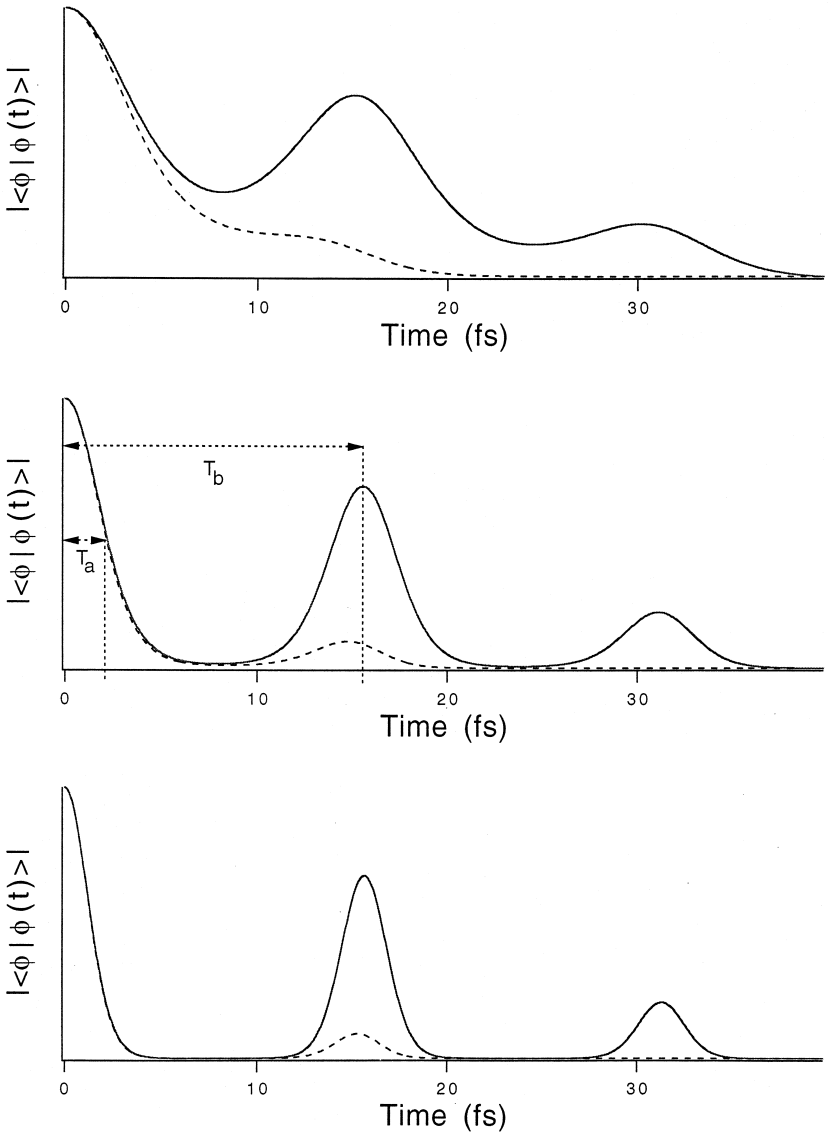

Fig. 2. Plot of the magnitude of the overlap versus time for a frequency of 400 cm^{-1} and for three different values of the distortion, Δ. The different values of the distortions are: top panel $\Delta = 1$, middle panel $\Delta = 2$ and bottom panel $\Delta = 3$. In all of the plots, dotted lines have a Γ of 100 cm^{-1} and solid lines have a Γ of 40 cm^{-1}. The magnitude of the recurrences would return to 1.00, but the damping factor, Γ, explained in text, causes the recurrences to eventually disappear.

necessary for the propagating wave to move away from its initial position and therefore diminish the overlap. The initial slope, and thus the time it takes for the overlap to decrease, will determine the broadness of our spectrum. A steep slope causes a rapid decrease in the overlap resulting in a small value of the time required for the overlap to decrease to half its initial value (T_a in Fig. 2). An event that requires a short time to occur in the time domain results, after Fourier Transform, in a high frequency (or energy) in the frequency domain. The breadth of the spectrum in the frequency domain is given by $2\pi/T_a$. The more aligned the minima of the two potential surfaces (ground and excited) are to each other, the smaller the slope of the surface on which the wave packet finds itself after the electronic transition, and the sharper the emission spectrum (because the wave packet moves away from its initial position slowly resulting in a large value of T_a in the time domain). As seen in Fig. 1, this 'alignment' of potential surfaces, or relative position of one from the other, is defined as the distortion Δ. A big value of Δ represents a big distortion in the excited state, and vice versa. In an experimental spectrum, the breadth allows us to calculate the size of Δ. A big Δ causes the initial wave packet (after the vertical transition) to end up on a steep slope. The steeper the slope, the sharper the drop, the broader the spectrum.

In Fig. 2, we have also indicated a second important time that we call T_b. It is the time it takes for the propagating wave packet to get back to where it started from, leading to a recurrence of overlap. The physical meaning of the recurrence in the overlap is the vibra-

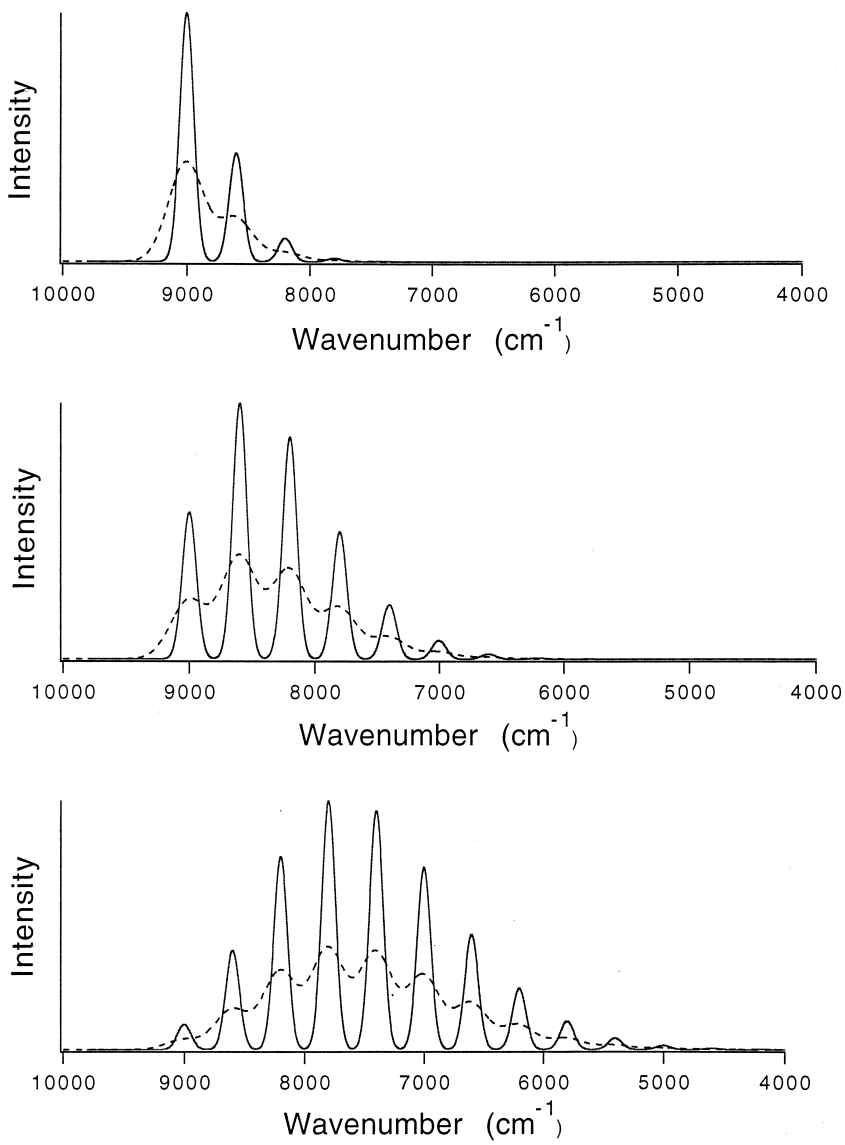

Fig. 3. Emission spectra calculated using the potential surfaces that give rise to overlaps in Fig. 2. The frequencies and distortions are the same as those in Fig. 2. In all of the spectra, dotted lines have a Γ of 100 cm^{-1} and solid lines have a Γ of 40 cm^{-1}. The emission spectra in each panel are normalized to equal area.

tional period of the vibrational normal mode, i.e., the time it takes for the oscillator to undergo one complete motion from its initial position, through the extreme of elongation or contraction, back to its initial position. For a harmonic oscillator, this time will remain the same each successive recurrence. It is translated into our spectrum, which is in the frequency domain, as the spacing between the different 'bumps' that constitute a progression. When we have only one dimension, and therefore only one frequency to determine the shape of our emission spectra, then we will only have one progression in that frequency. The spacing in wavenumbers between the distinct bumps (see Fig. 3) is constant and is given by $2\pi/T_b$.

The third important time that is included in our plot of $\langle \phi | \phi(t) \rangle$ is a mathematical function known as a 'damping factor' or Γ that is imposed on the overlap to damp its recurrences to represent the physical processes that cause the wave packet to leave the potential surface. These processes include transfer of amplitude to other electronic surfaces, the 'bath' or surrounding medium, etc. The damping factor is also frequently used to include all of the broadening mechanisms that can affect a spectrum including 'inhomogeneous broadening' caused by multiple emitting sites of slightly different energies in a liquid or solid. There are other more accurate ways to include inhomogeneous effects [15,16], but for simplicity we will lump everything into a 'phenomenological damping factor' Γ. The damping factor smears out individual peaks in the frequency domain, and sometimes is so big that we are unable to identify individual peaks at all. In Fig. 3, we illustrate how the different values of Γ change the appearance of the emission spectrum. With a small value, $\Gamma = 40$ cm^{-1}, the vibronic peaks are resolved to the baseline. When we use a bigger value, $\Gamma = 100$, there is less resolution of each vibronic peak, and they do not go down to the baseline.

Frequently, we cannot know from an emission spectrum alone the specific vibrations that our molecule possesses because the spectra are usually broadened. However, we can take advantage of another spectroscopic tool, resonance Raman, to determine which modes have displaced potential surfaces. The explanation of these processes deviates from the intent of this paper, and therefore will not be discussed, but the reader is referred to Refs. [5,15,17–20] to achieve a better understanding of their theoretical treatment and experimental applications.

3.2. Emission spectra with multiple vibrational modes

A molecule containing N atoms has $3N$-6 normal modes of vibration. Fortunately, not all of these modes will have displaced potential surfaces, and not all of the Δ's for those modes that are distorted will be large. However, the emission spectra of organometallic molecules usually encountered in the literature contain significant contributions from more than one normal mode. In this section, we expand on the above discussion by including additional vibrational modes. We begin by discussing the basic effects and illustrate our discussion with a two-mode example. We then show how the contributions of two or more modes can lead to spectra that could easily be misinterpreted. Finally, we show that inclusion of modes with small distortions does not change the picture very much, and that in fact their inclusion is in some respects similar to increasing the damping.

We begin with emission spectra from a two-mode example shown in Fig. 4. These spectra depict two different progressions, one with a vibrational frequency of 2000 cm^{-1} and the other of 300 cm^{-1}. Such frequencies are typical of a carbonyl stretch and a metal–ligand stretch. In the top panel of this figure we observe both progressions with relatively small distortions, $\Delta = 1$. This means that the minima of the potential surfaces are not that far away from each other, (in the horizontal axis), thus giving a slow decrease in overlap and a large value of T_b. Our choice of Γ lets us see a resolved spectrum with two clear progressions, one in each of the modes. The vibronic bands that create the first progression will have a constant separation of 300 cm^{-1}. The relative intensities of these bands, in this case where there is a small distortion, will decrease as we increase the quantum number, because the total width of the spectrum is small. We can see the progression in the 2000 cm^{-1} band, and in each quantum of the 2000 cm^{-1} mode there is a progression of the 300 cm^{-1} one. The intensities of the second progression of the 300 cm^{-1} mode are smaller because we are at a higher quantum level in the 2000 cm^{-1} mode. For each quantum in the biggest frequency, we can see all the quanta of the smallest frequency because, in this case, both frequencies are so far apart that we can see the progressions individually. Both progressions behave the same because they have the same distortion. When one of them has a noticeably different distortion than the other, then the relative intensities of the peaks change, as well as the number of peaks present for each progression (as we saw in Fig. 3 when we increased the Δ for a spectrum that consisted of only one mode). This can readily be observed in the next frame, where the biggest frequency, 2000 cm^{-1}, has a big distortion, Δ, relative to that of the lower frequency. The intensities of the peaks that form the progression change, resulting in the most intense peaks being farther from the first quanta of vibration. How far from it they are depends on the magnitude of Δ. As the distortion increases, the largest intensity will be found in higher vibrational levels because the total width of the spectrum is larger. In the third frame, the 2000 cm^{-1} mode has a small distortion

compared to that of the 300 cm^{-1} mode. Therefore, the relative intensities between the series of bumps that compose our progression in the biggest frequency remains the same as the first frame, namely: biggest, smaller, smallest. But now, the 300 cm^{-1} mode with a big distortion will have a different array of relative intensities among the peaks that constitute its progression, and in addition it has more vibronic bands (similarly to what happened in Fig. 3) because the total width is larger. Note that the relative intensities of the low frequency mode are always replicas of each other (scaled by the intensities of the peaks in the high-frequency mode.) This pattern is a signature of uncoupled normal coordinates. If the patterns change in the spectra, then coupling occurs, and a more detailed treatment is required. We will return to this point in Section 3.5.

To illustrate the applications of the above ideas to the interpretation of an experimental spectrum, consider the low-temperature emission spectrum of Ph_3PAuCl. In the course of our studies of the luminescence of gold-containing molecules [20,21], we measured the emission of Ph_3PAuCl. This emission has been previously reported [22], but the distortions have not yet been analyzed. Fig. 5 shows our experimental spectrum from an inorganic matrix at about 15 K (continuous line), and our fit calculated by using the time-dependent theory (dotted line).

To achieve a fit of an experimental spectrum, the first step is to find E_{00}, that is, the emission from the lowest vibrational level in the excited state potential surface to the lowest vibrational level in the ground-state potential surface. This band is the beginning of every

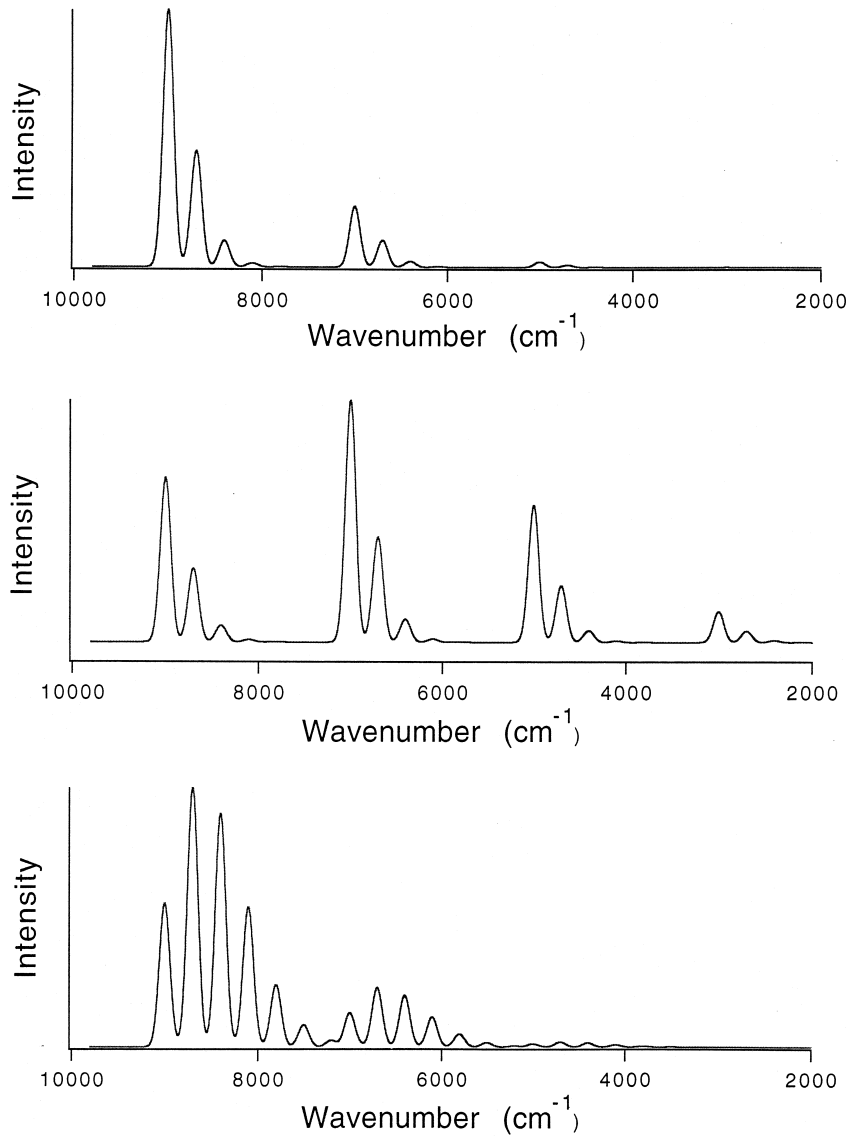

Fig. 4. Emission spectra with two displaced normal modes of frequencies 2000 cm^{-1} and 300 cm^{-1}. In the top panel both have the same distortion, $\Delta = 1$. In the middle panel, the frequency of the 2000 cm^{-1} mode has $\Delta = 2.5$ while the low frequency has $\Delta = 1$. In the bottom panel the high frequency has $\Delta = 1$ but the low frequency has $\Delta = 2$. All of the emission spectra were calculated with a Γ of 40 cm^{-1}.

progression, and its shape and size, in relation with all the other vibronic bands present, can give us some hints as to what our choice of Γ should be (individual width of this peak) and if the vibrational frequencies involved will have big distortions or not (compare its size to those of the other vibronic bands present in the spectrum). Once E_{00} is determined, we can measure the spacing between this peak and the others, and thus determine the vibrational frequencies of the displaced modes. In the case of Fig. 5 we can see that the first peak 300 cm^{-1} to lower energy is much smaller than E_{00}, which tells us that it will have a small distortion (for reasons similar to those underlying the progression in the 400 cm^{-1} mode in Fig. 3). This conclusion is verified by the even weaker intensity of the peak that represents the second quanta of the 300 vibration.

The next vibronic band to lower energy is bigger. Therefore, it is not part of the same progression, because, for the intensities to increase as we go to bigger quantum numbers, E_{00} must be the smallest of the peaks in the progression. In addition, the energy separation that corresponds to this peak (around 1090 cm^{-1}) is not three quanta of the first frequency. Continuing with this analysis, we can go through every vibronic band and assign its place in a particular progression. There is an independent check on the vibrational frequencies; a Raman spectrum of this molecule [22] has been obtained and similar frequencies are observed.

After the frequencies are determined and a semi-quantitative assessment of the distortions is made, the experimental spectrum is fit by making an initial guess at the Δ's, calculating the spectrum, comparing it with the experimental one, and varying the Δ's until the best fit between the spectra is obtained. The excellent quality of the fit shows that the spectrum is dominated by four normal modes. The calculated Δ's are given in the caption to Fig. 5.

3.3. The 'Beat' and the 'MIME'

When two or more distorted normal modes contribute to an emission spectrum, the complexity of the spectrum increases compared to a spectrum dominated by one mode. With large distortions and/or similar frequencies of the modes, progressions overlap. The analysis of the spectrum of Ph_3PAuCl discussed above shows how a spectrum can be systematically interpreted. Sometimes, however, the spectrum can look deceptively simple when in fact it is quite complex. Two such deceptive cases that we have discovered and named, the 'Beat' [23] and the 'MIME' [24–26], are discussed and analyzed in this section.

As the starting point for analysis of the deceptive examples, we will return to a two-mode example, this time with frequencies of 400 cm^{-1} and 600 cm^{-1} and both with $\Delta = 1$. The emission spectrum, shown in Fig. 6, is similar to that in Fig. 4 except that the progressions are overlapped because the frequencies are not as far apart from each other as in Fig. 4. In this spectrum, we cannot clearly distinguish between the two progressions because they are so close in frequency. When this happens, we may encounter several spectroscopic effects that may trick our eye and lead us in wrong directions when trying to assign the frequencies that compose our spectrum. Two of these features are shown in the second and third frames of Fig. 6. All three of the

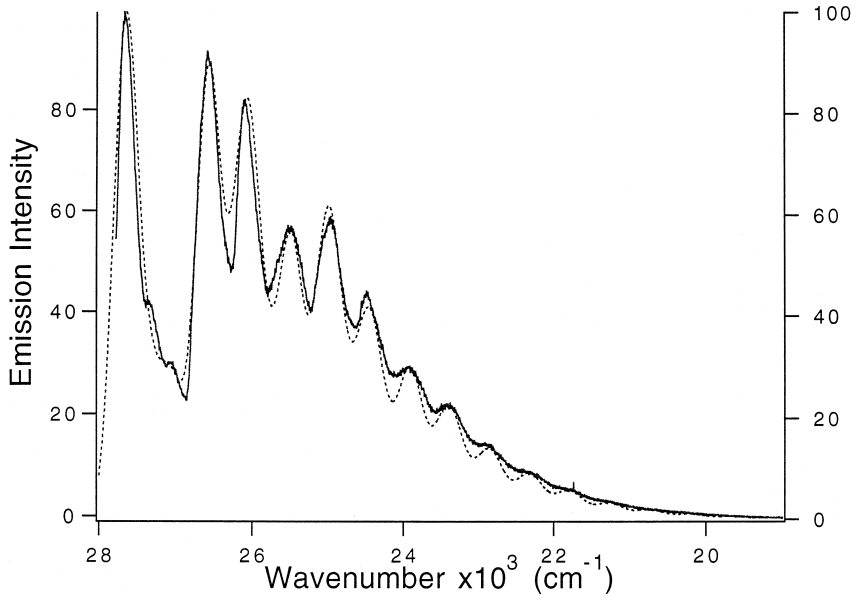

Fig. 5. Emission spectra of Ph_3PAuCl in an inorganic matrix taken at 15 K. The dotted line is the calculated fit to the spectrum using four modes ($\Gamma = 110$): 1083 cm^{-1} with $\Delta = 1.38$, 1580 cm^{-1} with $\Delta = 1.16$, 600 cm^{-1} with $\Delta = 0.7$ and 300 cm^{-1} with $\Delta = 0.7$.

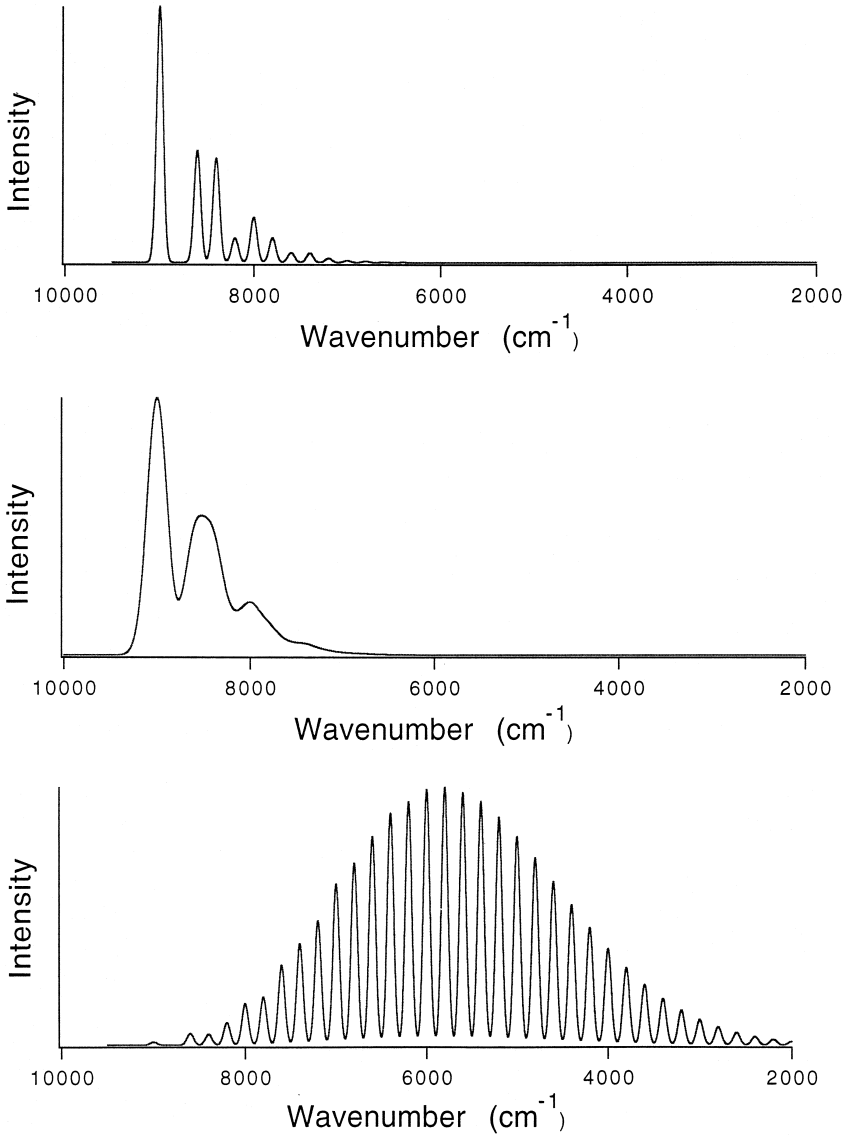

Fig. 6. Emission spectra calculated for 2 modes with similar frequencies (400 and 600 cm^{-1}). These spectra show how the interplay between distortions and damping drastically changes the appearance of the spectra. Top panel: both frequencies have a $\Delta = 1$ and a small Γ ($\Gamma = 25$). Middle panel: the MIME, same frequencies as top panels but Γ is bigger ($\Gamma = 75$). Lower panel: the Beat, same frequencies as above panels, but larger distortions $\Delta = 3$ in both normal modes with $\Gamma = 25$.

spectra contain only two modes with frequencies of 400 and 600 cm^{-1}.

In the second frame, we can see how increasing Γ broadens the individual peaks, smearing them into wide peaks (which might happen experimentally), and giving an impression that there is just one progression with a frequency of 500 cm^{-1}. This is what is called the Missing Mode Effect or 'MIME' because the spectrum mimics one progression [24–26]. The origin can be easily understood from the overlap in the time domain (Figs. 7 and 8). The top of Fig. 7 shows the overlap with a small Γ, which, after Fourier transformation, gives the spectrum in the top panel of Fig. 6. When Γ is bigger, it diminishes the overlap before we can get enough recurrences. Only the recurrence at $T_b = 11$ fs dominates, and therefore the Fourier Transform gives us a progression with a frequency $2\pi/T_b = 500$ cm^{-1} that is a compromise between the frequencies involved. The reason that the compromise frequency is observed can be seen from the top two panels of Fig. 8. The total overlap is the product of the top two panels; the maximum of the product overlap is between the maxima at about 16 fs for the low frequency peak and that at 10 fs for the high-frequency peak. When a large Γ 'kills' the overlaps at longer times, only the compromise overlap remains. Note that the compromise overlap will be between the maxima of the constituent overlaps, but is not a simple arithmetic average of the two [26]. This effect was first discovered in the emission spectrum of the organometallic molecule $W(CO)_5$pyridine.

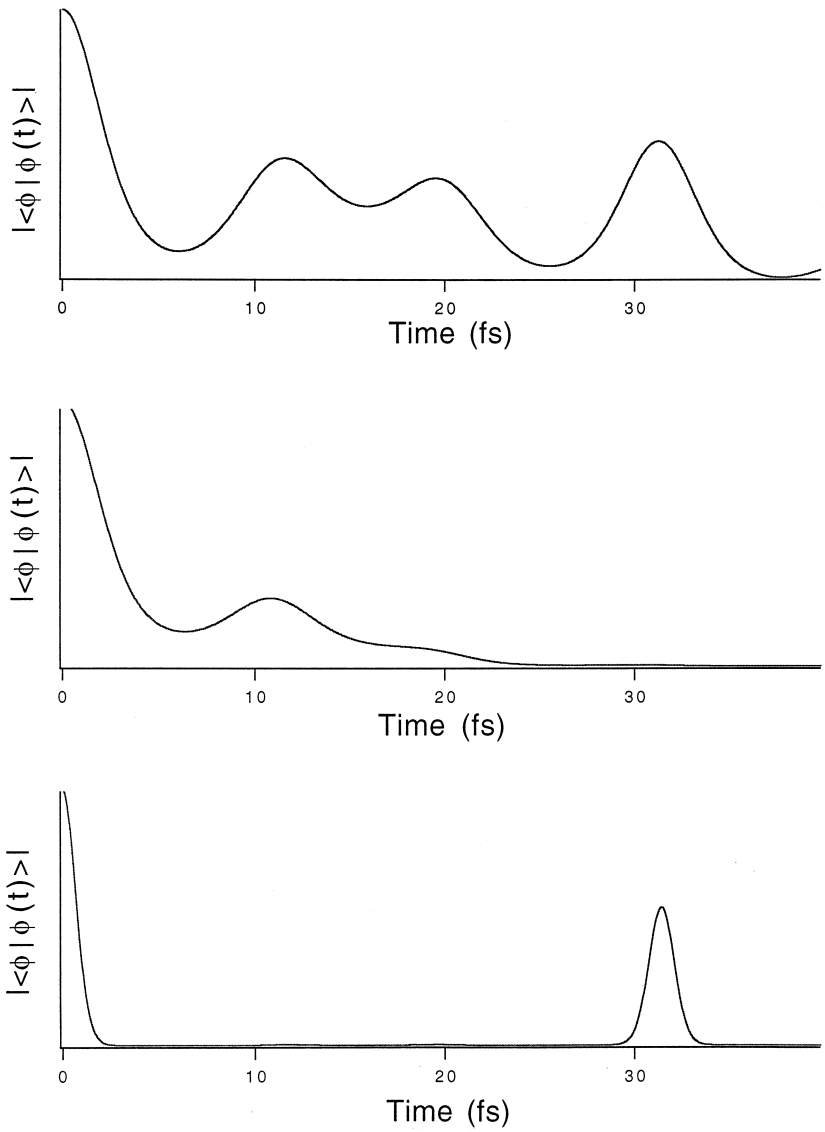

Fig. 7. Plot of the magnitude of the overlap versus time for the two mode spectra shown in Fig. 6. The frequencies of vibrations and the values of the distortions (Δ's) and Γ's are the same as in Fig. 6.

The third frame of Fig. 6 shows what appears to be a spectrum caused by a large distortion in a single 200 cm^{-1} mode. However, this effect, called the Beat, is actually also composed of two frequencies of 400 and 600 cm^{-1}, but this time with large distortions. Because both distortions are big, both progressions will have a maximum intensity near the middle of their respective progressions, but the individual peaks that constitute these progressions will only be 200 wavenumbers apart from each other in the spectrum. Note that the distance between the lowest quanta (E_{00}) and the first one is 400 cm^{-1}, because that is the smallest frequency of the two. From then on we will have the first quanta of the 600 cm^{-1} mode, and then the second of 400 cm^{-1} (800 cm^{-1} apart from E_{00}), then the first quanta of one with the second of the other, and so on, appearing to the eye as a progression in the 200 cm^{-1} mode with a big distortion. The key to discovering this type of progression is finding E_{00}, then assessing the spacing between it and the first vibronic band. This will be the lowest frequency. Any other progression that seems to be occurring at a frequency lower than that is just a result of two or more frequencies present in our spectrum.

In the time domain (Fig. 8), we can clearly see the cause of the apparent 200 cm^{-1} progression. The product of the overlaps of the 400 cm^{-1} (top) and 600 cm^{-1} (middle) modes is very large at about $T_b = 32$ fs where they coincide, but is very small at shorter times because the peak of one occurs at a valley of the other. The Fourier transform of the bottom panel will give a spectrum that has a vibronic spacing of $2\pi/T_b = 200$ cm^{-1}. This explanation is akin to a beat frequency in classical

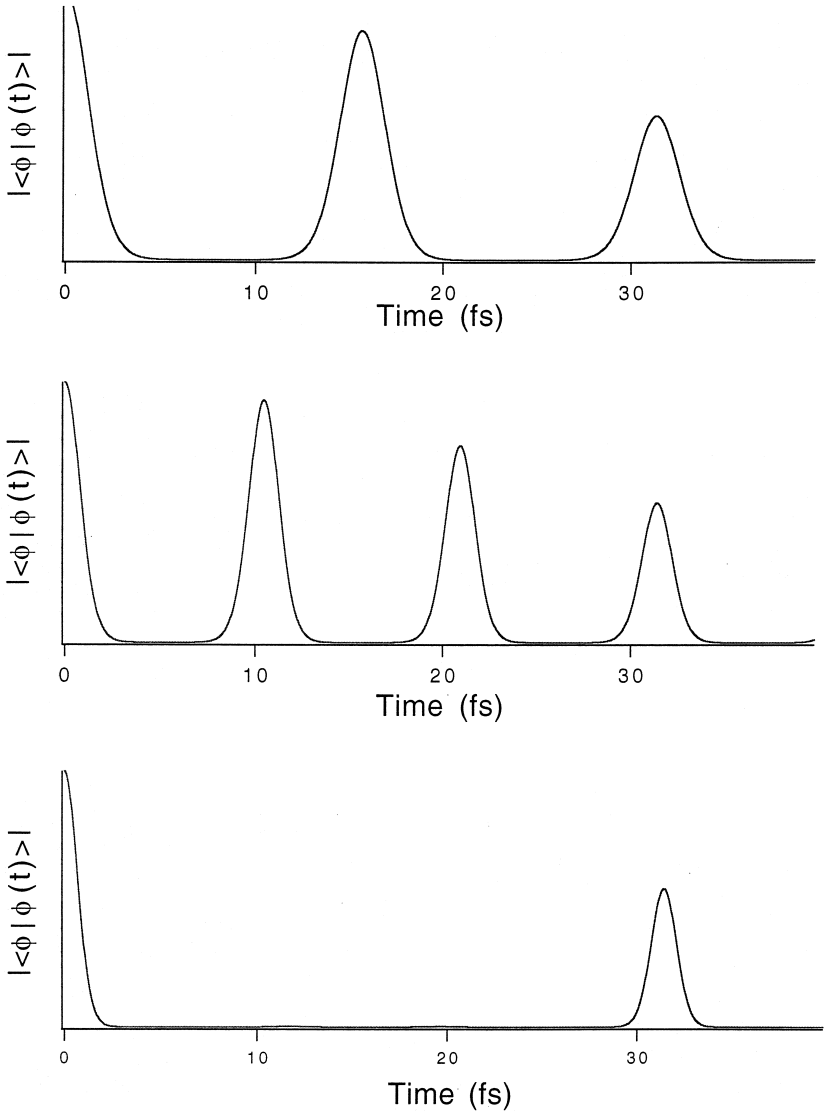

Fig. 8. Plot of overlap versus time illustrating the Beat for frequencies of 400 and 600 cm^{-1}. The top panel shows the overlap of only the 400 cm^{-1} mode. The middle panel shows it for the 600 cm^{-1} mode. The bottom panel is the product of these two overlaps. Note that the only major recurrence occurs at about 32 fs. When the product overlap is Fourier transformed, the emission spectrum appears to have a vibronic progression in a 200 cm^{-1} vibration.

physics where two waves of different frequencies combine to give a beat frequency that is the difference between the two original frequencies.

We conclude this section with experimental examples of the MIME and the beat in the emission spectra of metal compounds. The spectra of *trans*-$W(N_2)_2(dppe)_2$ (dppe = 1,2 bis(diphenylphosphino) ethane) provide an excellent example of the MIME [27]. The emission spectrum taken at 80 K is shown in the middle panel of Fig. 9. It appears to contain a single progression with a spacing of 500 cm^{-1}. Lowering the temperature to 10 K resolves new features (Fig. 9, top panel). In the low-temperature spectrum, these vibronic peaks correspond to metal–nitrogen (524 cm^{-1}) metal–phosphine (176 cm^{-1}) and a variety of phenyl ring modes (1000–1500 cm^{-1}). The calculated low-temperature spectrum is given by the solid line in the middle panel. It was calculated with a Γ of 17.5 cm^{-1}. The emission spectrum of the 80 K sample is calculated using *exactly* the same parameters of frequencies and distortions, but with a Γ of 80 cm^{-1} (Fig. 9, middle panel.) The larger γ kills longer time recurrences in the time domain, leaving just one recurrence at a 'compromise' time that, when Fourier transformed, corresponds to the 500 cm^{-1} MIME frequency observed in the frequency domain spectrum. In this example, more than the two modes that contribute the spectra in Fig. 6 are involved, but the explanation of the effect is the same.

The emission spectrum of $((C_2H_5)N)_2[Pd(MNT)_2]$ $(MNT = S_2C_2(CN)_2)]^-$ provides a good example of the Beat [28]. The spectrum, shown in Fig. 9 (bottom

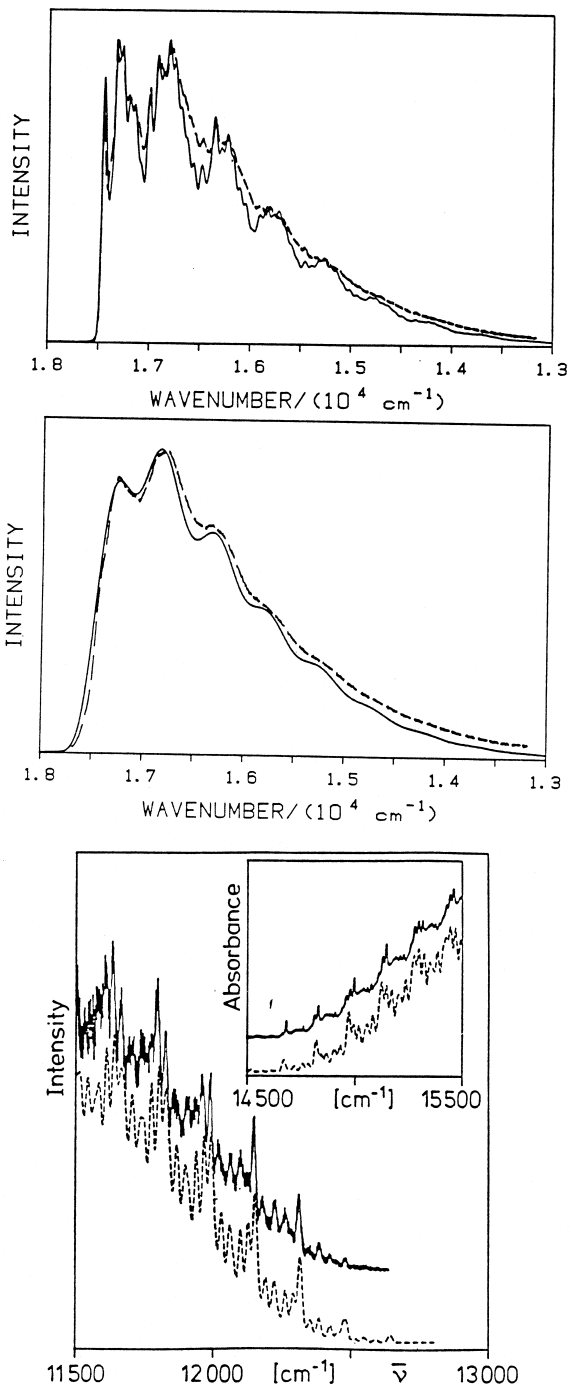

Fig. 9. Top and middle: the emission spectra (dotted lines) of *trans*-$W(N_2)_2(dppe)_2$ (dppe = 1,2 bis(diphenylphosphino)ethane). The spectrum taken at 80 K, shown in the middle panel, appears to contain a single progression with a spacing of 500 cm^{-1}. Lowering the temperature to 10 K resolves new features (top panel). The calculated low temperature spectrum ($\Gamma = 17.5$ cm^{-1}) is given by the solid line in the middle panel. The emission spectrum of the 80 K sample is calculated using *exactly* the same parameters of frequencies and distortions but with a Γ of 80 cm^{-1} (middle panel.) Bottom: the emission spectrum of $((C_2H_5)N)_2[Pd(MNT)_2]$ (mnt = $S_2C_2(CN)_2)^{2-}$. The regular 26 cm^{-1} spacing between the vibronic features is the beat frequency between the two most highly distorted modes in the molecule (162 cm^{-1} and 188 cm^{-1}).

panel), contains a regular 26 cm^{-1} spacing between the vibronic features. The 26 cm^{-1} frequency is the beat frequency between the two most highly distorted modes in the molecule (162 cm^{-1} and 188 cm^{-1}). In this example, the emission band containing the beat overlaps another (unstructured) band to lower energy and only the high energy side of the spectrum is shown. The calculated example in Fig. 6 shows the entire band. In both cases, the product overlap contains a big recurrence at long times which, when Fourier transformed, gives rise to the low-frequency beat frequency in the spectrum.

3.4. Effect of multiple modes with small distortions

Sections 3.2 and 3.3 examined the effects of more than one mode with specific examples of two distorted modes. The addition of more modes results in more complexity in the emission spectra, but the patterns that develop follow the principles that we have described for the new patterns resulting from adding a second mode to the one-mode case. Spectra are calculated and fit to experiment by including the appropriate overlaps in the product overlap (Eq. (5)).

A common occurrence in many molecules is that a small number of modes have large distortions and the remainder have very small distortions. In such cases, the spectrum is dominated by the highly distorted modes and the remainder merely act like a damping factor. In this section we briefly analyze and explain this result.

The most important effect of increasing the number of modes with small distortions is the broadening of the spectrum. This effect is illustrated in Fig. 10, where the top panel shows a spectrum with just one mode with a large $\Delta = 3$, and the bottom panel shows the spectrum with additional modes with frequencies of 100, 200 and 2000 cm^{-1} and Δ's of 1. In both spectra, the value of Γ, the damping factor, is the same (80 cm^{-1}.) The bottom spectrum appears to be less well resolved than the top spectrum. The time domain explanation of the apparent loss of resolution is contained in the overlap. Inclusion of modes of different frequencies means that the recurrences of these modes will happen at different times. Specifically, the recurrence of the highly distorted mode will happen when the overlaps for the other modes are small, and thus in the product overlap, the total recurrence at that time will be smaller. This decrease is similar to the decrease caused by increasing the damping. The relative intensities of the vibronic bands is not strongly affected; thus fitting the bottom spectrum with just one mode and a larger damping factor would yield a calculated distortion not very different from that calculated with all of the modes. The approximate calculation (not all of the modes, larger damping) is frequently not a bad approximation, and distortions determined in this manner will frequently not

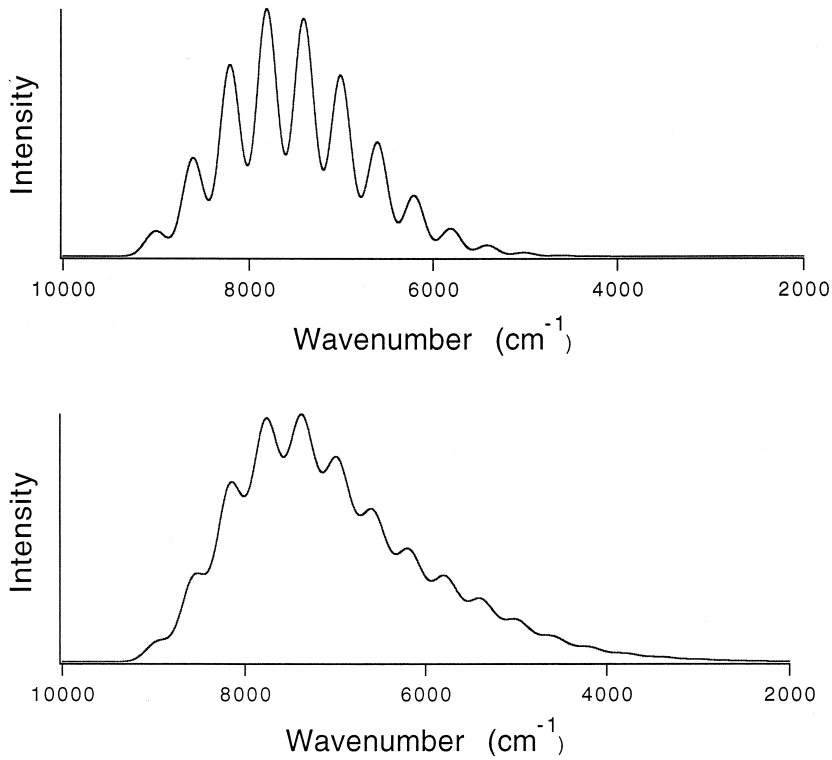

Fig. 10. Emission spectra illustrating how adding modes with small distortions acts like the damping factor. Top panel shows the calculated spectra containing one 400 cm^{-1} mode and $\Delta = 3$. The lower panel has the same mode as the top one, and additional modes with frequencies of 100, 200 and 2000 cm^{-1} all of which have $\Delta = 1$. Both spectra are calculated with a damping factor $\Gamma = 80$ cm^{-1}.

be far wrong. However, it will always be more accurate to include all of the displaced modes using information from resonance Raman spectra.

The overall width of the emission spectrum is dominated by the steepest slope of the multidimensional potential surface. For a specific normal mode, the greater the distortion, the larger the slope, and for a given distortion, the greater the vibrational frequency the larger the slope. Thus, if one particular mode is very highly distorted and the remainder of the modes have very small distortions, the initial decrease in the overlap will be dominated by the slope of the highly distorted mode, and the other modes will only have a small effect. Thus, the width of the spectrum and the calculated distortion for the highly distorted mode will not be drastically changed by the inclusion of other modes with small distortions. This result is also illustrated in Fig. 10. Note that the width at half height is about the same. The inclusion of the high-frequency mode does cause a noticeable tailing to lower energy; although its distortion is small, the slope is appreciable because of the high frequency.

3.5. Coupled vibrational normal modes

In this section, we return to the case of two displaced modes with very different vibrational frequencies such that the progressions are separated from each other as shown in Fig. 4. The emission spectrum of hexafluoroacetylacetonatodimethylgold(III), Me_2Auhfac, shown in Fig. 11, at first glance appears to fit the description of a spectrum dominated by a low frequency and a high-frequency mode [29]. There are clusters of bands whose individual peaks are separated by 262 cm^{-1}. These clusters are separated from each other by 1352 cm^{-1}. However, the clusters in Fig. 11 are not replicas of each other like they are in Fig. 4. Instead, the intensity distribution of peaks in each cluster changes; each cluster to higher energy of the previous one has an intensity distribution in which the lower energy peaks of the cluster gain intensity relative to the higher energy peaks. The 'non-replica' pattern cannot be accounted for by uncoupled potential surfaces, and requires a surface where the two modes (both totally symmetric) are coupled.

The uncoupled potential 'best fit' to the $(n, 0)$ progression between 21 000 and 23 000 cm^{-1} is obtained by using $\Delta_x = 1.57$, $\Delta_y = 1.5$, and frequencies of 1352 cm^{-1} and 262 cm^{-1}, respectively (Fig. 11, top). Although a good fit to the $(n, 0)$ progression is obtained, the fits of the $(n, 1)$, $(n, 2)$ etc. progressions are poor. The reason for the poor match is the increase of the width of the low frequency progression with increasing quantum number of the high frequency mode, (i.e., the progressions are not replicas of each other).

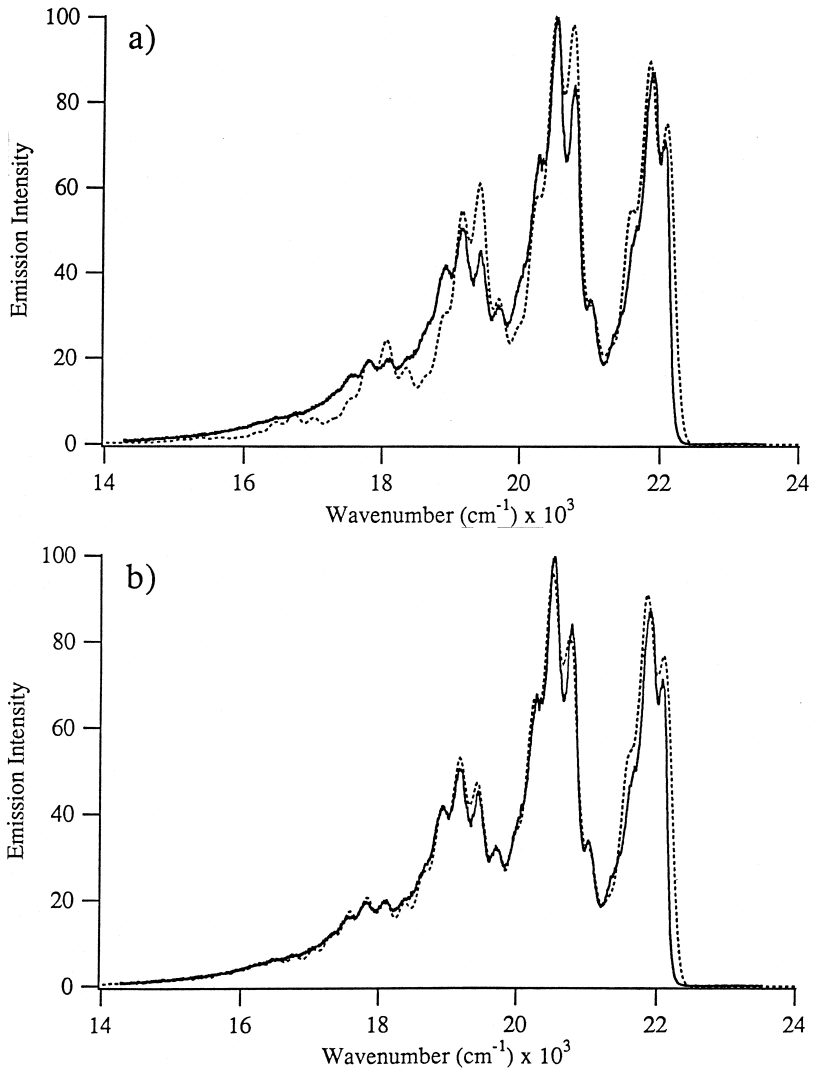

Fig. 11. The 15 K emission spectrum of hexafluoroacetylacetonatodimethylgold(III) (solid lines). The top panel show the 'best fit' with uncoupled normal modes (dotted lines.) The bottom panel shows the best fit with quadratically coupled normal modes ($\Gamma = 74$ cm^{-1}, 258 cm^{-1} with $\Delta_x = 1.44$, 1354 cm^{-1} with $\Delta_y = 1.52$ and a coupling between the modes of $k_{xy} = 116.5$ cm^{-1}).

The best fit between the experimental and calculated spectra is shown in the bottom of Fig. 11. The values of the parameters for the transition to ground state potential are: $E_{00} = 22\,910$ cm^{-1}, $\Gamma = 74$ cm^{-1} $\Delta_x = 1.44$, $\Delta_y = 1.52$ with frequencies of 258 cm^{-1} and 1354 cm^{-1} respectively, and a coupling between the modes of $k_{xy} = 116.5$ cm^{-1}.

The 'non-replica' pattern of bands is a spectroscopic signature of normal mode coupling. When coupling occurs, the wave packets do not move independently on cross-sections of the multidimensional potential surface. Instead, the motion in one of the dimensions is influenced by the position of the wave packet in a different dimension. When evidence for such coupling is encountered in an experimental spectrum, more detail about the excited-state structure can be extracted than from an uncoupled spectrum. However, unless the coupling is very large, a good first approximation of the excited-state distortions can be obtained by obtaining the best fit to the spectrum using uncoupled surfaces (in the above example, the largest error is less than 10%).

4. Coupled electronic states

Up to now, we have described and calculated emission spectra of organometallic compounds in a two electronic state picture (the ground state and one excited state). This model is frequently a good approximation. However, it is just an approximation because in most molecules there are many excited states lying relatively close in energy (such that the absorption bands overlap, for example). In these cases, coupling between the states (spin–orbit coupling, for example) may be significant and may be different at different internuclear geometries. Coupling between electronic states can eas-

ily be included in the time-dependent theory. We have developed the theoretical description for several important types of coupling and explored their spectroscopic ramifications [30–37]. Three effects, briefly discussed in this section, are particularly important in organometallic photochemistry and photophysics: intensity borrowing, intersystem crossing and electron transfer. A fourth, interference dips (related to 'Fano antiresonance') is more of an oddity but may cause confusion. All four are very closely related; we briefly describe each of them and provide references to the original literature for more detailed derivations and discussion.

4.1. Intensity borrowing

The electronic spectra of organometallics form a rich area for investigating the effects of potential surface coupling because one of the important sources of state coupling, spin–orbit coupling, is large and because frequently many excited electronic states with different displacements and force constants lie relatively close together in energy. One of the most important spectroscopic consequences of spin–orbit coupling is 'intensity borrowing' in which a formally spin-forbidden transition 'borrows' or 'steals' intensity from a spin-allowed transition. The appearance of spin-forbidden transitions is frequently explained in this way [38,39]. Another important consequence of spin–orbit coupling is unexpected vibronic structure. Progressions in a vibrational normal mode may be induced in forbidden transitions, or the relative intensities of the members of a progression may take on unusual patterns. These effects may reveal themselves in the band envelopes in unresolved spectra, or most interestingly, in the vibronic bands themselves in resolved spectra.

In the time-domain picture, amplitude transfer between surfaces due to coupling can cause a spin-forbidden transition to gain intensity in the electronic spectrum [31,32,35]. A forbidden transition means that the initial wave packet is multiplied by zero (the transition dipole moment) and thus does not have any amplitude on the potential surface called 'surface 1' with spin multiplicity different from that of the ground state. However, for the spin-allowed transition, the wave packet is multiplied by the nonzero transition dipole moment, and the wave packet is transferred vertically from the ground state onto the potential surface (called 'surface 2'.) When spin–orbit coupling between the two states is nonzero, amplitude is transferred from surface 2 to surface 1. The rate at which the wave packet develops amplitude is related to intersystem crossing, and the population is related to the intensity that is borrowed.

The trends in the emission intensity distributions in the vibronic structure induced by coupling between excited-state potential surfaces can be interpreted from the trends in the eigenfunction of the lowest energy vibrational level of the coupled excited states, i.e., the initial wave packet at $t = 0$. The initial wave packet consists of two parts, one from the part of the eigenfunction associated with surface 1 multiplied by the transition dipole between surface 1 and the ground state, and the second part from the part of the eigenfunction associated with surface 2 multiplied by the transition dipole between surface 2 and the ground state.

The spectra calculated by propagating the above functions on a harmonic ground state potential are shown in Fig. 12. For zero coupling, there is no emission spectrum because the transition is dipole-forbidden. As the coupling increases, the intensities of the vibronic side bands relative to that of the origin increase. A simple physical picture for explaining the increasing intensity of the side bands to that of the origin is that the wave packet has increasing probability at a position away from the minimum of the ground-state surface giving rise to more rapid decreases in $\langle \phi | \phi(t) \rangle$, hence to a broader spectrum containing more vibronic features (in the time-independent picture, the initial eigenfunction appears to be more and more displaced leading to better overlap with higher quanta vibrational wavefunctions of the ground electronic state).

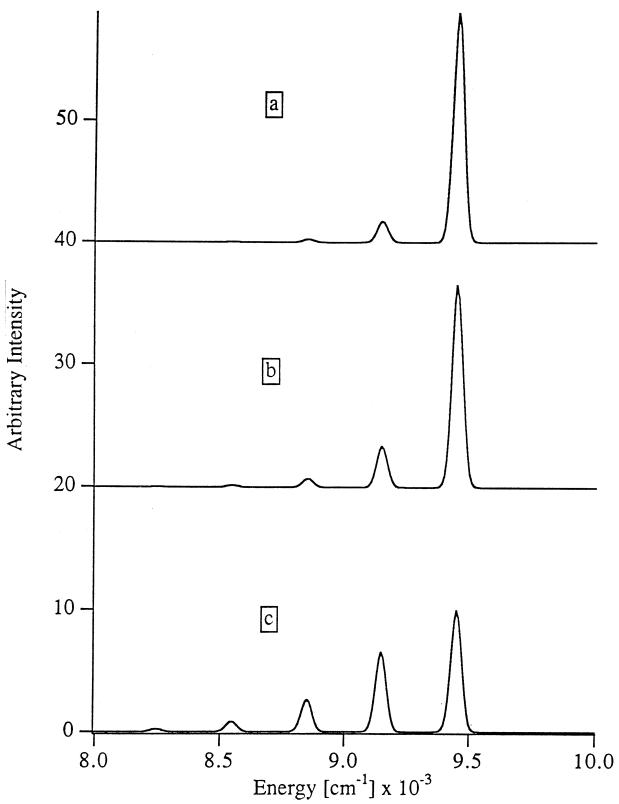

Fig. 12. 'Forbidden' emission spectra from an undisplaced potential surface coupled to an allowed state. The coupling constants are (top to bottom) 500, 1000 and 3000 cm^{-1}.

The net results of increasing the excited state potential surface coupling are to allow the spin-forbidden transition, and to induce a vibronic progression in the emission from an undisplaced potential surface. The magnitudes of these effects depend, not only on the coupling, but also on the relative placements of the potential surfaces. Although the trends can be understood in terms of the physical pictures discussed above, case-by-case quantitative calculations must be carried out to understand the details in the spectra of specific molecules.

Quantitative analysis of resolved vibronic structure in the emission spectra of manganese(V) in oxide lattices using the theory described above has been reported [35]. Short progressions are observed in totally symmetric Mn–O modes although no distortions are expected. These experimental results provide a rigorous test because the input parameters are precisely measured. The calculated intensities of the vibronic bands in the spectra are in excellent agreement with the measured values.

4.2. Interference dips (Fano antiresonance)

Another spectroscopic effect caused by coupling of electronic states is an unexpected decrease in intensity where the spectra of two states overlap. When electronic states are uncoupled, the spectrum consists of the sum of the individual spectra from the states, but when the states are coupled, the resulting spectrum may not be the simple sum but instead can contain dips (loss of intensity). The origin of the dips is destructive interference between the wave packet moving on one of the surfaces with the wave packet moving on the coupled surface. We have called this phenomenon 'interference dips' and quantitatively treated them in the spectra of metal compounds [30]. They are related to 'Fano antiresonance' in atomic spectroscopy.

The time-domain explanation of an interference dip is found in the overlap. When the two surfaces are coupled, the total overlap decreases more rapidly than in the uncoupled case. In addition, the overlap then increases to give a small recurrence and then slowly decreases again. In contrast, the overlap for the uncoupled surfaces decreases smoothly to zero. The initial decrease is less rapid than that calculated with coupling. The more complicated behavior of the overlap with coupling is explained by the population changes that take place. The population of diabatic surface 2 rapidly decreases, reaches a local minimum, and then increases to reach a local maximum. The initial decrease corresponds to loss of population to diabatic surface 1 followed by net back transfer of some population. The overlap roughly follows the population, although its magnitude is not simply proportional to the population because the properties of the wavefunction are changed when the population changes. When compared to the overlap for the uncoupled case, the decrease is more rapid at a short time but a recurrence is also observed. When transformed to the frequency domain, the more rapid decrease results in a broader spectrum, i.e., in more intensity at higher energies and less intensity at lower energies in the spectrum relative to that in the uncoupled case. The small recurrence results in a feature at $c^{-1}\ t_{\text{recurrence}}^{-1}$ in the frequency domain. The net result of these two effects is to produce a spectrum for the coupled case in which a dip is observed in the envelope. Interference effects, large or small, always occur between two potential surfaces when the surfaces are coupled.

4.3. Electron transfer

Our final set of examples that illustrate the importance of coupling between electronic states involves electron transfer. Many different types of electron transfer have been studied spectroscopically including metal-to-metal, ligand-to-ligand, and intervalence electron transfer [1–4,40,41]. In all of the cases that are relevant to our discussion, the initial and final electronic states are coupled, a photon causes electron transfer, and the system relaxes with back electron transfer. When the initial and final surfaces have minima at different energies and internuclear separations, the theoretical treatment requires wave packet hopping (amplitude transfer) between the surfaces as discussed above [19]. In the case of intervalence electron transfer, the surfaces have minima at the same energies but at different internuclear separations [33,37].

An intervalence absorption spectrum represents an interesting and subtle type of electronic transition where the initial and final states cannot be represented by potential energy surfaces and the Born–Oppenheimer approximation [33,37,42]. The intervalence absorption band is a low-energy transition in the red or near-IR region of the absorption spectrum that is present in molecules containing two interchangeably equivalent sites with different oxidation states, but is absent in molecules where the two sites have the same oxidation state [40,41]. A large number of examples are known where the two sites are metal atoms connected by a bridging ligand. We have examined three different pairs of diabatic surfaces representing three different models that generate the same adiabatic potential surfaces [37]. Each of these three models is based on a different physical picture of the intervalence transition. The first model represents charge transfer between two sites, the second represents a transition between bonding and antibonding molecular orbitals, and the third represents a nonbonding to nonbonding transition. We derived the specific forms of the couplings required to give the adiabatic potential energy surfaces and the transition dipole moments, and calculated the spectra for each

model. The details of these models are outside of the scope of this paper, but the physical picture provided by wave packet dynamics and the role of excited state distortions in determining the spectra are understandable in terms of the principles discussed earlier in this paper.

5. Summary

The time-dependent theory provides a powerful quantitative calculational method and intuitive physical picture for interpreting the dynamics of a molecule after absorption or emission of a photon. In this paper we showed the connections between the motion of the wave packet on a potential surface and the corresponding luminescence spectrum. Other photophysical processes are interpreted in terms of wave packet transfer between coupled surfaces. The changes in bond lengths and bond angles can be calculated, and a picture of the molecule in the lowest excited state can be obtained.

Acknowledgements

This work was made possible by a grant from the National Science Foundation (CHE 95-09275).

References

[1] A.W. Adamson, P.D. Fleischauer (Eds.), Concepts of Inorganic Photochemistry, Wiley, New York, 1975.
[2] G.L. Geoffroy, M.S. Wrighton, Organometallic Photochemistry, Academic Press, New York, 1979.
[3] J. Sykora, J. Sima, in: A.B.P. Lever (Ed.), Photochemistry of Coordination Compounds, Vol. 107, Elsevier, Czechoslovakia, 1990.
[4] D.M. Roundhill, Photochemistry and Photophysics of Metal Complexes, Plenum, New York, 1994.
[5] J.I. Zink, K.-S. Kim Shin, in: D.H. Volman, G.S. Hammond, D.C. Neckers, Advances in Photochemistry, Vol. 16, Wiley, New York, 1991.
[6] A.J. Lees, Chem. Rev. 87 (1987) 711.
[7] M. Kasha, Discuss. Faraday Soc. 9 (1950) 14.
[8] E.J. Heller, Acc. Chem. Res. 14 (1981) 368.
[9] E.J. Heller, J. Chem. Phys. 68 (1978) 3891.
[10] E.J. Heller, J. Chem. Phys. 68 (1978) 2066.
[11] M.D. Feit, J.A. Fleck, A. Steiger, J. Comp. Phys. 47 (1982) 412.
[12] D. Kosloff, R. Kosloff, J. Comp. Phys. 52 (1983) 35.
[13] J.J. Tanner, J. Chem. Educ. 67 (1990) 917.
[14] H. Yersin, H. Otto, J.I. Zink, G. Gliemann, J. Am. Chem. Soc. 102 (1980) 951.
[15] A.B. Myers, Chem. Rev. 96 (1996) 911.
[16] K.-S. Kim Shin, J.I. Zink, J. Am. Chem. Soc. 112 (1990) 7148.
[17] K.-S. Shin, R.J.H. Clark, J.I. Zink, J. Am. Chem. Soc. 111 (1989) 4244.
[18] K.-S. Kim Shin, R.J.H. Clark, J.I. Zink, J. Am. Chem. Soc. 112 (1990) 3754.
[19] J.L. Wootton, J.I. Zink, J. Phys. Chem. 99 (1995) 7251.
[20] S.D. Hanna, J.I. Zink, Inorg. Chem. 35 (1996) 297.
[21] S.D. Hanna, S.I. Khan, J.I. Zink, Inorg. Chem. 35 (1996) 5813.
[22] L.J. Larson, E.M. McCauley, B. Weissbart, D.S. Tinti, J. Phys. Chem. 99 (1995) 7218.
[23] J.I. Zink, C. Reber, Coord. Chem. Rev. 111 (1991) 1.
[24] L. Tutt, D. Tannor, E.J. Heller, J.I. Zink, Inorg. Chem. 21 (1982) 3859.
[25] L. Tutt, D. Tannor, J. Schindler, E.J. Heller, J.I. Zink, J. Phys. Chem. 87 (1983) 3017.
[26] L.W. Tutt, J.I. Zink, E.J. Heller, Inorg. Chem. 26 (1987) 2158.
[27] L.J. Larson, J.I. Zink, Inorg. Chem. 28 (1989) 3519.
[28] W. Gunter, G. Gliemann, H. Kunkely, C. Reber, J.I. Zink, Inorg. Chem. 29 (1990) 5238.
[29] D. Wexler, J.I. Zink, J. Phys. Chem. 97 (1993) 4903.
[30] C. Reber, J.I. Zink, J. Chem. Phys. 96 (1992) 2681.
[31] C. Reber, J.I. Zink, Comments Inorg. Chem. 13 (1992) 177.
[32] D. Wexler, C. Reber, J.I. Zink, J. Phys. Chem. 96 (1992) 8757.
[33] E. Simoni, C. Reber, D.S. Talaga, J.I. Zink, J. Phys. Chem. 97 (1993) 12678.
[34] D. Wexler, J.I. Zink, C. Reber, in: H. Yersin (Ed.), Electronic and Vibronic Spectra of Transition Metal Complexes, Springer, Berlin, 1994, p. 174.
[35] D. Wexler, J.I. Zink, Inorg. Chem. 34 (1995) 1500.
[36] J.L. Wootton, J.I. Zink, J. Phys. Chem. 99 (1995) 7251.
[37] D.S. Talaga, J.I. Zink, J. Phys. Chem. 100 (1996) 8712.
[38] C.J. Ballhausen, Introduction to Ligand Field Theory, McGraw-Hill, New York, 1962.
[39] H.L. Schlaefer, G. Gliemann, Basic Principles of Ligand Field Theory, Wiley, London, 1969, p. 96.
[40] D.B. Brown (Ed.), Mixed Valence Compounds, Reidel, Dordrecht, 1980.
[41] M.B. Robin, P. Day, Adv. Inorg. Radiochem. 10 (1967) 247.
[42] S.B. Piepho, E.R. Krausz, P.N. Schatz, J. Am. Chem. Soc. 100 (1978) 2996.